Springer

KSME

Journal of Mechanical Science and Technology 30 (7) (2016) 3347~3356
www.springerlink.com/content/1738-494x(Print)/1976-3824(Online)
DOI 10.1007/s12206-016-0644-1

Improvement of collection efficiency and solar fraction in solar thermal storage system using a 3-way valve and a 2-stage flowrate control †

Jong Hyun Kim[1], Uk Jae Lee[1], LongJie Li[1], Chul Kim[2] and Hiki Hong[2,*]

[1]*Department of Mechanical Engineering, Graduate School, Kyung Hee University, Yongin 446-701, Korea*
[2]*Department of Mechanical Engineering, Kyung Hee University, Yongin 446-701, Korea*

(Manuscript Received August 1, 2015; Revised February 19, 2016; Accepted March 18, 2016)

Abstract

In the present study, we investigated the effects of a combined system-control method in a solar thermal system; specifically, prevention of temperature reversal plus a reduced circulation rate. A 3-way valve is adopted as a remedy of the temperature reversal in the water storage tank and a 2-stage flowrate is implemented as the flowrate control strategy. To evaluate the effects, we perform five experiments and TRNSYS based simulations with a carefully developed system-control algorithm. As the main result, we experimentally validated that a 3-way valve is effective for the prevention of temperature reversal and a 2-stage flowrate extends the solar energy collection time. Annual simulation results show that the proposed combined method improves the system performances (1.9%p increase of collector efficiency, 2.2%p increase of solar fraction, and 5.3% additional collected energy) compared to the conventional forced circulation system. Our results should be applied to the water storage tank proposed in this study.

Keywords: Solar thermal system; Stratification; Temperature reversal; 2-stage flowrate control; TRNSYS; Collection efficiency; Solar fraction

1. Introduction

Solar thermal systems convert the solar energy into thermal energy and store it in the form of heated water which can be used during a later time. They are recognized as some of the most competitive systems in the renewable energy field due to their high economic feasibility and availability [1]. As for the technology of the water storage tank, the thermal stratification inside the tank is widely acknowledged as the means by which the overall system performance is improved as the collector inlet temperature decreases. Regarding this, previous studies reported that the stratification improves the useful energy consumption by 5-20% [2, 3]. Further, other experimental and theoretical studies showed that stratification enhancement technology, which increases the temperature difference between the top and bottom of the storage tank, results in a higher collection efficiency and higher exergy [4-10].

In the conventional forced circulation system employing pumps, antifreeze is circulated in a closed loop between the collector and the heat exchanger located inside the storage tank in order to prevent freezing during the winter season. The collected thermal energy is transferred through the heat exchanger, and is then stored inside the storage tank. Storage tanks employed in small or medium-sized solar systems utilize the internal heat exchange coil to minimize the overall system size. In such systems, the heat exchange coil is usually installed between the middle and bottom of the storage tank. Contrary to this lower installation of heat exchange coil, our previous studies showed that the upper and side heating of the storage tank is more effective for higher stratification performance [11], as upper heating increases the temperature difference between the top and bottom of the storage tank. However, a drawback of upper heating arises when the solar irradiation condition is poor. In this case, the upper temperature of the storage tank is observed to be higher than the collector's outlet temperature; we call this phenomenon temperature reversal. Consequently, temperature reversal destroys the stratification since the thermal energy stored in the upper side is transferred to the lower side through the flow inside the exchange coil.

We already proposed a novel method to prevent the temperature reversal [12, 13]. In those studies, the whole heating coil inside the tank was divided into the upper coil and the lower coil, and the antifreeze returning from the collector usually circulated through the whole coil. When the temperature sensors detected the temperature reversal, the antifreeze circulation was rearranged to pass through only the lower coil by adopting a 3-way valve. The effect of this novel idea was confirmed by an experiment and a simulation based on TRNSYS

*Corresponding author. Tel.: +82 31 201 2928, Fax.: +82 31 202 2625
E-mail address: hhong@khu.ac.kr
† Recommended by Associate Editor Jae Dong Chung

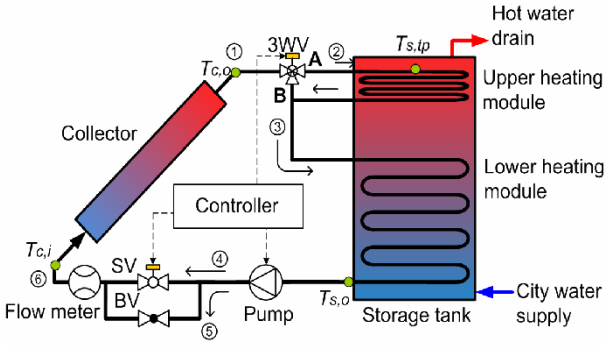

Fig. 1. Schematic of the experimental set-up of the solar combi-system. 3WV: 3-way valve, SV: Solenoid valve, BV: Bypass valve

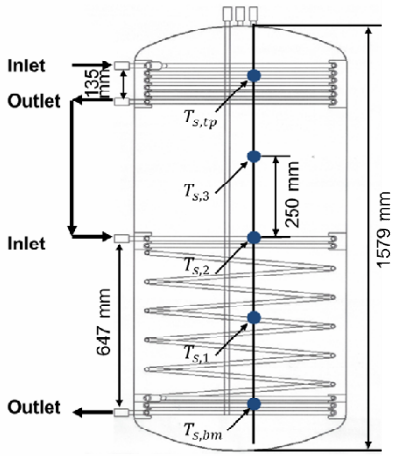

Fig. 2. Drawing of the storage tank. Solid circles represent the thermocouple positions.

[12]. Another critical parameter affecting the stratification performance is the circulating flowrate. A previous study [14] showed that the well-controlled forced system shows a better performance than the natural system, which utilizes buoyancy as the driving force of circulation. The natural circulation, however, showed a higher performance when the irradiation condition was poor. This interesting point can be explained as follows. Under poor irradiation, the natural circulation still collects the energy even though the flowrate is low. On the other hand, the forced system, which operates under the predetermined operating condition, stops the energy collection when it encounters poor irradiation. This analysis suggests that the elaborate control of flowrate can improve the system performance, even in with poor irradiation. However, this means an additional installation cost in the small- or medium-sized systems is necessary if a precise flowrate control such as the inverter control is implemented.

In this study, we investigate the system performance for the combined system, which integrates the flowrate control into the prevention of temperature reversal. Here, we introduce a 2-stage flowrate control method, which usually operates with normal flowrate in the good irradiation condition and switches to a low flowrate under a poor irradiation condition. In particular, this simple 2-stage flowrate control is designed to be cost competitive. From a theoretical point of view, the low flowrate lowers the collection efficiency compared to the normal flowrate, but increases the collector's outlet temperature. This increase in temperature is supposed to be useful for stratification enhancement in the storage tank and a higher solar fraction. In addition, low flowrate is expected to extend the collection time.

As the outline of this study, we conducted five experiments (Modes 1-5) to verify the effects of lower heating, upper heating, temperature reversal prevention and low flowrate. However, it is not feasible to compare the system performance for the above five modes only through short time experiments since the actual daily meteorological condition is not repeated exactly. In this regard, we evaluate the system performance for the five modes using a commercial code (TRNSYS) under a given meteorological condition.

2. Experiment

2.1 Experimental setup

Fig. 1 shows the schematic of the experimental setup for a solar thermal system composed of a collector, a storage tank and a controller. First of all, we explain the closed loop connected in a series by the collector, 3-way valve, upper heating module, lower heating module, pump, solenoid valve, bypass valve and flow meter. The antifreeze (Propylene glycol 40% + Water 60% by weight) circulation through this loop collects solar energy on the collector and stores the thermal energy in the tank through the heating modules, where three control units (pump, 3-way valve, solenoid valve) adjust the loop according to the control signals. The pump is controlled by an ON/OFF mechanism; ON means the system is turned on and OFF means the system is turned off. The 3-way valve determines whether or not the antifreeze circulates through the upper heating module (for example, open A and closed B means circulation through the upper heating module). An open solenoid valve makes the flowrate normal, whereas a closed solenoid valve makes the flowrate low since the bypass valve is always open.

Fig. 2 shows the drawing of the cylindrical storage tank (outer diameter: 750 mm, height: 1579 mm) used in the experiment. The upper heating module made of stainless pipe (outer diameter: 15.88 mm, thickness: 1.22 mm, length: 12 m, heat transfer area: 0.60 m^2, coil pitch: 27 mm) is installed in the upper part of the storage tank. The lower heating module (length: 20 m, heat transfer area: 1.0 m^2, coil pitch: 105.4 mm, the same stainless pipe as the upper heating module) is installed in the lower part of the storage tank. The short coil pitch of the upper side enhances a locally intensive heat transfer compared to the lower side, so that the upper side temperature will increase more quickly than the lower side. Specifications for the four main components of the system (collector, storage tank, heating coil, pump) are listed in Table 1.

Temperatures were measured using a thermocouple (K-

Table 1. Specifications of the system.

Collector	Size	1180 × 2400 mm^2
	Area	2.83 m^2 × 4
	Slope	45°
Storage tank	Capacity	550 L
	Material	STS304
Heating coil	Upper	15A × 12 m
	Lower	15A × 20 m
	Material	STS304
Pump	Capacity	35 lpm (H : 3 m)
	Output	40 W

type) at four points ($T_{c,i}$, $T_{c,o}$, $T_{s,o}$, $T_{s,tp}$) for system monitoring and control, as shown in Fig. 1, and at five points ($T_{s,bm}$, $T_{s,1}$, $T_{s,2}$, $T_{s,3}$, $T_{s,tp}$) inside the storage tank (see Fig. 2) along the tank axis at an interval of 250 mm in order to obtain the temperature profiles. Flowrate was measured using a turbine flowmeter (FLOW-300, 0.5-15 lpm, accuracy ±1.0%, ILJIN) while irradiation was recorded using a pyranometer (MS-602, ISO 9060 Second Class, sensitivity ±2%, EKO). All the data were gathered using a data logger (HP34970A, Agilent) at intervals of 12 seconds.

2.2 Five experiment modes (Modes 1-5)

In mode 1, the lower heating module in the storage tank is heated with the normal flowrate. The antifreeze flows along the loop (① → B of 3-way valve → ③ → lower heating module → pump → ④ and ⑤ → flow meter → ⑥ → collector → ①) (see Fig. 1). In the normal flowrate, a small portion of the normal flowrate occurs through the path (⑤ → bypass valve) in parallel with the path of (④ → solenoid valve). Mode 1 is considered to be the conventional heating method. In mode 2 [12], antifreeze flows with the normal flowrate along the loop (① → A of 3-way valve → upper heating module → ③ → lower heating module → pump → ④ and ⑤ → flow meter → ⑥ → collector → ①) (see Fig. 1). Thermal stratification is expected to be enhanced in this mode since intensive heat transfer occurs in the upper side. Mode 3 is identical to mode 2 regarding the usual condition. However, when the temperature reversal occurs, the 3-way valve stops the circulation of the upper heating module to form the loop in mode 1. Consequently, the heat transfer from the upper side to the lower side is prevented. In this regard, the upper side temperature is expected to maintain a constant temperature. Mode 4 is also usually operated as in mode 2. However, under the condition of poor irradiation, the flowrate is changed into the low state by closing the solenoid valve to form the loop (① → A of 3-way valve → upper heating module → ③ → lower heating module → pump → ⑤ → bypass valve → flow meter → ⑥ → collector → ①) (see Fig. 1). Hence, the collector's outlet temperature should increase due to the lowered flowrate. Mode 5 is the proposed method which combines modes 3 and 4. Theoretically estimated performances of the five modes are summarized in Table 2.

Table 2. Expected performances of five modes.

Mode	Control	Degree of stratification	Prevention of temperature reversal	Operation under bad irradiation period
Mode 1	LH	×	○	×
Mode 2	LH + UH	Δ	×	×
Mode 3	LH + UH + 3WV	Δ	○	×
Mode 4	LH + UH + 2SF	○	×	○
Mode 5	LH + UH + 3WV + 2SF	○	○	○

LH: Lower heating, UH: Upper heating, 3WV: 3-way valve, 2SF: 2-stage flowrate. ○: Good, Δ: Normal, ×: Bad

2.3 Algorithm of system control

In this study, the algorithm of system control is important in order to adequately realize the benefits of the combined method. The system control is carried out based on the temperature difference (ΔT) between the collector's outlet temperature ($T_{c,o}$) and the tank's outlet temperature ($T_{s,o}$), $\Delta T = T_{c,o} - T_{s,o}$. Normal flowrate ($\dot{m}_{nor}$) was determined to be 0.17 kg/s based on our previous experiments. This flowrate allows the usual ΔT to be maintained around 10 K in the good irradiation condition. As a result of this flowrate, the temperature difference between the outlet and inlet of the collector is kept higher than the difference between the top and bottom of the storage tank. Hence, system control is stabilized and frequent system ON/OFF changes do not occur. The system ON/OFF condition was determined from our previous experiments; ΔT_{on} (from OFF to ON) was set to 12 K, ΔT_{off} (from ON to OFF) was set to 2 K.

As already mentioned, we employed a 2-stage flowrate control composed of the normal flowrate $\dot{m}_{nor}$ and the low flowrate $\dot{m}_{low}$, which is set to one fifth of $\dot{m}_{nor}$ (= 0.034 kg/s, $\dot{m}_{low} = \dot{m}_{nor}/5$). The switchover from $\dot{m}_{nor}$ to $\dot{m}_{low}$ occurs if ΔT decreases to 3 K. On the other hand, the switchover from $\dot{m}_{low}$ to $\dot{m}_{nor}$ occurs if ΔT increases up to 15K. The rationale for the above 15 K, 3 K and the relation of $\dot{m}_{low} = \dot{m}_{nor}/5$ can be explained as follows. The switchover from $\dot{m}_{nor}$ to $\dot{m}_{low}$ should occur at a temperature that is higher than the temperature for system OFF. If 1 K of margin is added to 2 K (system OFF temperature), 3 K is obtained. Thus, the tank's outlet temperature is usually very close to the collector's inlet temperature ($T_{s,o} \approx T_{c,i}$). Therefore, a quantitative relation for ΔT ($\approx T_{c,o} - T_{c,i}$) is expressed as follows, using the two relations for the collector: the energy collection rate $\dot{Q} = \dot{m} C_p \Delta T$ and the definition of collector efficiency $\eta = \dot{Q} / (A_c I_t)$.

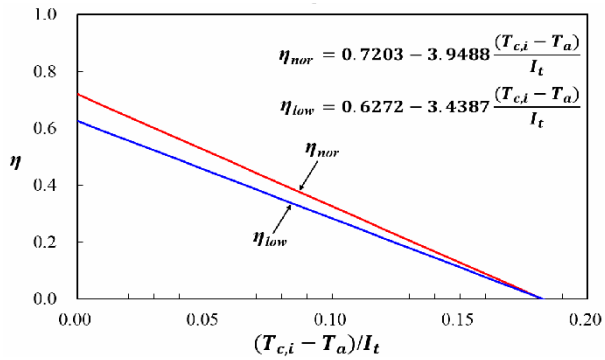

Fig. 3. Collector efficiency curves.

$$\Delta T = \frac{\eta A_c I_t}{\dot{m} C_p}. \quad (1)$$

Therefore, the ΔT ratio between the low and normal states, leads to the following equation for the given A_c, I_t and C_p:

$$\frac{\Delta T_{low}}{\Delta T_{nor}} = \frac{\eta_{low}}{\eta_{nor}} \frac{\dot{m}_{nor}}{\dot{m}_{low}}. \quad (2)$$

The ratio η_{low}/η_{nor} in the above equation can be obtained from the following equation expressing the collector efficiency [13]:

$$\eta = F_R(\tau\alpha) - F_R U_L \frac{(T_{c,i} - T_a)}{I_t}. \quad (3)$$

For the normal flowrate, the experimental values for the collector used in our experiment are 0.7203 for $F_R(\tau\alpha)$ and 3.9488 for $F_R U_L$. Using collector theory [16], we can calculate $F_R(\tau\alpha)$ as 0.6272 and $F_R U_L$ as 3.4387 for the low flowrate. The two efficiencies of η_{nor} and η_{low} exhibit a linear relation with respect to $(T_{c,i} - T_a)/I_t$, plotted in Fig. 3, and η_{low}/η_{nor} is 0.871 over the entire range. Subsequently, by inserting $\eta_{low}/\eta_{nor} = 0.871$ and $\dot{m}_{low} = \dot{m}_{nor}/5$ into Eq. (2) for ΔT_{nor} = 3 K, we get 13.1 K for the value of ΔT_{low}. This result implies that the switchover temperature 3 K ($\dot{m}_{nor} \rightarrow \dot{m}_{low}$) for the normal flowrate is equivalent to 13.1 K for the low flowrate. Now, the other switchover temperature ($\dot{m}_{low} \rightarrow \dot{m}_{nor}$) should be greater than 13.1 K in order to prevent the immediate return from $\dot{m}_{low}$ to $\dot{m}_{nor}$. In this context, considering a margin, we decided a switchover temperature from the low flowrate to the normal flowrate of 15 K to avoid frequent switchovers between the two flowrates.

As the control criteria for the prevention of temperature reversal, both the upper heating module and the lower heating module are circulated if $T_{c,o}$ is greater than $T_{s,tp}$. Otherwise, only the lower heating module is circulated.

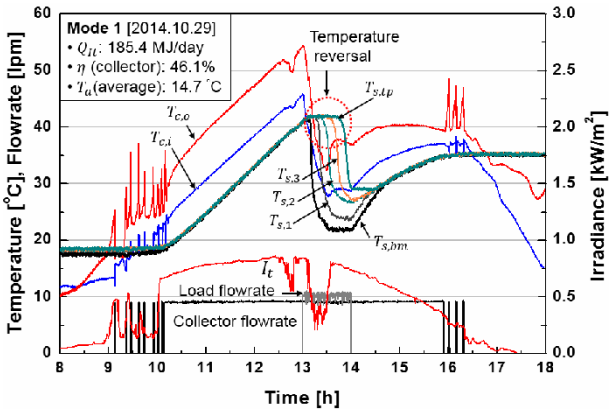

Fig. 4. Experiment results of mode 1 with load.

3. Experimental results and analysis

Experiments were carried out in the test site located at Kyung Hee University (Yongin, Korea) since September 2014 either in the good irradiation condition (clear day) or in the poor irradiation condition (cloudy day). Each experiment was carried out over one full day. To reflect a practical user's condition, a simple load scenario (hot water consumption of about 11 lpm during 1 hour from 13:00, total 660 L) was applied during the experiment for good irradiation; cold city water was supplied into the bottom of the storage tank while the same amount of hot water was drained from the top (see Fig. 1).

Fig. 4 shows the experimental results of mode 1. It discloses the measured flowrate, irradiation and temperature profiles from the early morning to the late afternoon. The initial pump operation between 9:00 and 10:00 shows frequent pump ON/OFF changes, which is a typical pattern of conventional forced solar water heating systems. The temperatures of the top ($T_{s,tp}$) and bottom ($T_{s,bm}$) of the tank are almost the same up to 13:00, showing a fully mixed state inside the storage tank. All temperatures during the load period (13:00-14:00) sharply drop due to the cold water supply. Although a temperature difference exists between $T_{s,tp}$ and $T_{s,bm}$, it is worth noting that a temperature reversal (dotted circle) occurs due to the sudden deterioration of irradiation (13:00-13:30). Thereafter, the temperatures rise again and return to the fully mixed state.

In mode 2, shown in Fig. 5, a notable stratification is obviously observed over the entire period for the experiment (see the difference between $T_{s,tp}$ and $T_{s,bm}$ profiles). In contrast to the perfect mixing of mode 1, this stratification is attributable to the effect of the intensive upper heating method. Furthermore, irregular irradiation generates temperature reversal (12:00-13:00, dotted circle). In the same manner as mode 1, the load initiation on 13:00 results in the sudden decrease of all temperatures. However, for the load time with good irradiation, temperature reversal is not observed. Considering the temperature reversal of modes 1 and 2, it can be concluded that temperature reversal occurs more frequently with poor irradiation.

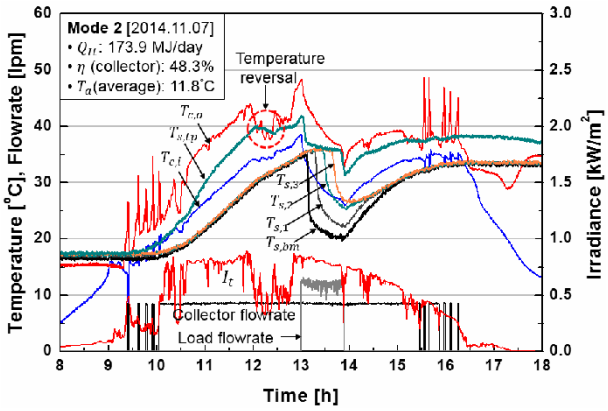

Fig. 5. Experiment results of mode 2 with load.

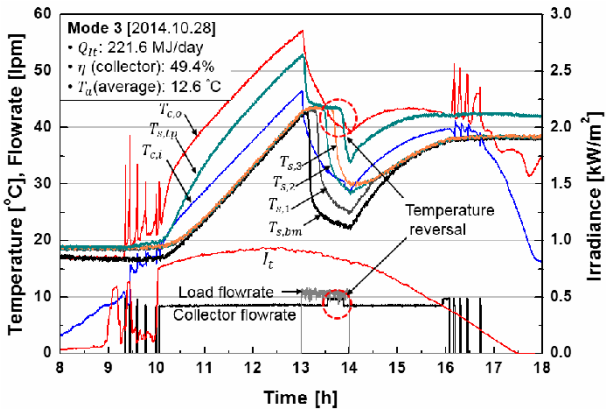

Fig. 6. Experiment results of mode 3 with load.

Fig. 6 shows the experimental results for mode 3 under the good irradiation condition. We can observe temperature reversal during the time interval between 13:30-14:00 (upper dotted circle). Interestingly, a small increase of flowrate is observed during this same interval (inside the lower dotted circle). In the circulation loop of mode 3, antifreeze flows into the lower heating module without passing through the upper heating module. Therefore, the flowrate increases due to the reduction of flow resistance since the total path is shortened. This means that our system control using a 3-way valve is correctly functioning. It is notable that the top temperature of the storage tank is maintained at an almost constant temperature (green line inside the upper dotted circle), as expected.

Fig. 7 shows experimental results of mode 4 carried out under the poor irradiation condition without load. As expected, the flowrate changed from $\dot{m}_{nor}$ to $\dot{m}_{low}$ under very low irradiation (comparing the low flowrate $\dot{m}_{low}$ between 12:00-13:00 and the normal flowrate $\dot{m}_{nor}$ between 11:00-12:00). This result clearly shows that our 2-stage flowrate strategy with the previously described control method can extend the energy collection time, even in the poor irradiation condition. Furthermore, we can observe the temperature reversal between 12:00-13:00 (see the dotted circle). Poor irradiation once again causes the temperature reversal. However, the upper temperature of the tank (green inside the dotted circle) slightly decreases during the interval of temperature reversal, which implies that the 3-way valve did not stop circulation in the upper heating module.

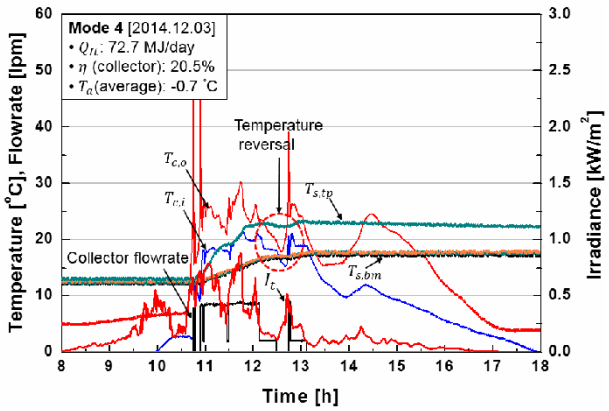

Fig. 7. Experiment results of mode 4 without load.

Mode 5 is the method that integrates the advantages of mode 3 (prevention of temperature reversal) and mode 4 (extension of energy collection time). Fig. 8 shows the experimental results of mode 5 for the clear day without load (Fig. 8(a)), clear day without load (Fig. 8(b)) and cloudy day with load (Fig. 8(c)). Mode 5 repeats the switchovers between the low and normal flowrates identified in mode 4 (Fig. 8(a): 9:30-10:30 and 14:00-15:30; Fig. 8(b): 9:30-10:00 and 15:30-16:30; Fig. 8(c): 11:30-12:30, 13:30-14:00, 14:30-16:00). These observations indicate that the advantages of mode 4 are effective mainly in the morning and afternoon, as well as for the deteriorated irradiation condition at noon. On the other hand, for the modes without the 2-stage flowrate control, only sporadic energy collection is observed in the poor irradiation condition (Fig. 4 of mode 1: 9:00-10:30 and 16:00-16:30; Fig. 5 of mode 2: 9:30-10:00 and 15:30-16:30; Fig. 6 of mode 3: 9:00-10:00, 16:00-17:00); series of thin spikes represent a short collection time. These results provide more evidence supporting the advantages of a 2-stage flowrate. Quantitative data analysis supports the above observations. Mode 5, shown in Fig. 8(a), shows a much higher additional energy collection compared to the conventional mode 1, shown in Fig. 4; 5.7 MJ of additionally collected energy for mode 5 (8.6% of the total collected energy) for mode 5, and 2.0 MJ of additional collection for mode 1 (1.8% of the total collected energy). In addition, Fig. 8 provides evidence for the preventive mechanism against the temperature reversal phenomena. In the time interval between 14:30-15:00 (Fig. 8(c)), a sudden deterioration of irradiation causes temperature reversal (see the dotted circles). In the profile for the flowrate, a small square on the green line indicates that the 3-way valve stopped circulation in the upper heating module. Fig. 8(c) presents the operation with the low flowrate and the temperature reversal prevention for the time interval 14:50-15:50. During this period, the top temperature of the storage tank maintained a constant temperature of 31°C, while the bottom temperature increased from 23.5°C to

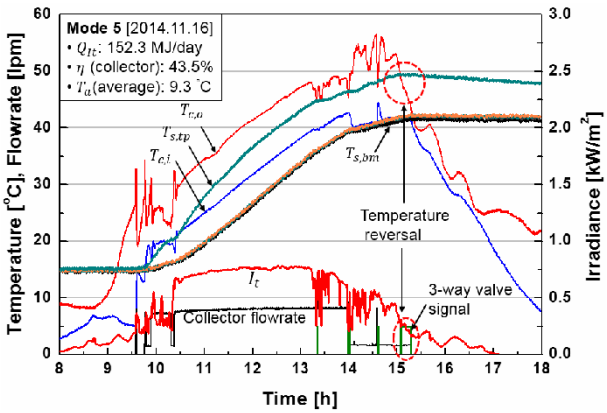

(a) Clear day without load

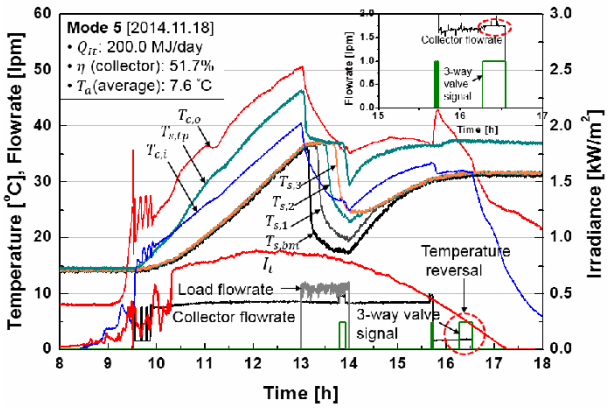

(b) Clear day with load

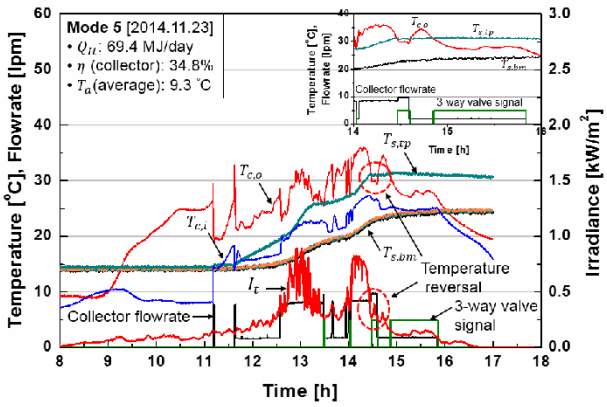

(c) Cloudy day without load

Fig. 8. Experiment results of mode 5.

24.3°C (see the upper inset). Further, the inset of Fig. 8(b) reveals that the low flowrate slightly increased, indicating that temperature reversal prevention has occurred (see the dotted upper ellipse). As a result, $T_{s,tp}$ maintains a constant temperature. We can find the same results for the 3-way valve in Fig. 8(b) (13:30-14:00 of load time, 16:00-16:30 in the late afternoon) and Fig. 8(c) (14:30-16:00 in the afternoon). Temperature reversal occurs more frequently in the afternoon.

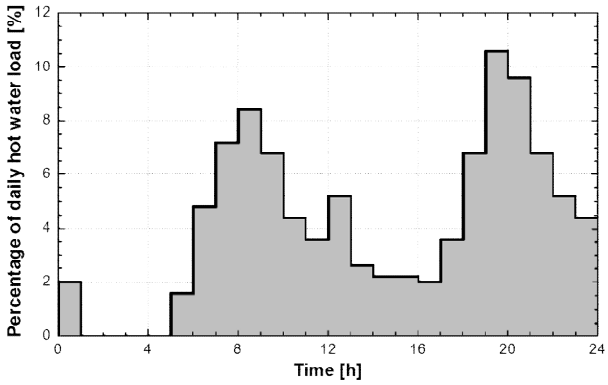

Fig. 9. Daily load pattern.

4. Simulation

4.1 Simulation process and modeling

Simulations were carried out using TRNSYS. First, measured meteorological data were input through the type 9c Data Reader module. The output data from the type 16a module, which produces the solar angle and solar radiation, were input into the type 1b collector module. The storage tank module of type 60d including two heat exchangers (the upper and lower heating modules) employed a simplified cylindrical model, where a stratified storage tank with 10 nodes was assumed. In the same manner as the experiment, the temperature difference between the collector outlet and inlet was used to control the system operation (Type 2b).

Commercial code EES was utilized to adjust the load temperature, circulated flowrate and city water flowrate. To reflect a practical user's condition, a load scenario, such as a hot water consumption of 650 L per day, was included in the simulation. The load pattern proposed by Cardinale et al. [17] (see Fig. 9) was used for the daily load pattern. Also, the city water temperature was adjusted to the month-averaged earth temperature (1.5 m below the earth) provided by the local Meteorological Administration.

The 3-way valve was implemented using type 11f. EES data were called from TRNSYS through a type 66b module, which calls external programs. After getting further information from TRNSYS (operation time from type 14h), EES calculates the flowrate of the city water upon receiv-ing the month-averaged city water temperature from type 518. The city water temperature and flowrate are then transferred to type 11h. The low flowrate mode and normal flowrate mode are input through type 2b. A signal (signal: 0 ~ 1 → flowrate: 0% ~ 100%) of type 2b is transferred to type 3b, which is then adjusted to the flowrate of the circulation pump.

The simulation was performed with time steps of 0.1 h and 0.01 h, however the results were almost identical.

4.2 Comparison between experiment and simulation

In order to evaluate the suitability of the preceding simula-

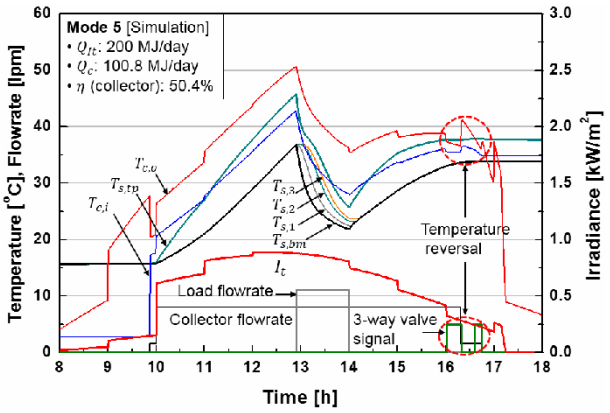

Fig. 10. Simulation result for mode 5 under the same condition as the experiment of Fig. 8(b).

tion, we compared the results from the experiment (Fig. 8(b)) and the simulation (Fig. 10) for mode 5 based on the data from 18th November 2014 (clear day, a load of 660 L from 13:00 to 14:00). The collector efficiency is 51.7% (= 103.4/200.0 MJ) for the experiment and 50.4% (= 100.8/200.0 MJ) for the simulation. The simulation shows 1.3%p lower efficiency than the experiment. Average temperatures of city water and atmosphere were 16.8°C and 7.6°C, respectively. The heat load (58.0 MJ) measured during the experiment was set as the input for the simulation.

The profiles (temperature, flowrate, irradiance) plotted in Fig. 8(b) and Fig. 10 show good overall agreements between experiment and simulation. They show similar circulation pump operating patterns. However, some partial discrepancies are observed in the temperature profiles between the top and bottom inside the storage tank. Although the first temperature reversal (13:40-14:00) observed in the experiment is not shown in the simulation, the second and third reversals (15:40-16:30) observed in this experiment are shown in the simulation at 16:30. These disagreements were expected since we could not completely reflect the complex structure of the storage tank and meteorological conditions in the modeling process. We performed an additional four simulations and compared the results with the experimental ones (not shown here). Those simulation results agreed well with the experiments regarding several aspects, such as pump ON/OFF. However, our simulation was revealed to be imperfect due to the imprecise simulation of actual irradiation. In other words, the hour-based irradiation curve in our simulation could not express the exact irradiation curve. We believe that a more accurate program is necessary for improved agreements.

4.3 Comparison of daily simulation results

We examined the performances of modes 1 and 5 using the foregoing simulation method under the same condition using the load pattern presented in Fig. 9, based on SAREK's Seoul standard meteorological data on 28th March and the initial storage tank temperature of 30°C.

Table 3. Summary of daily simulation results for modes 1 and 5.

	Mode 1	Mode 5
Solar radiation [MJ]	240.2	
Collected heat [MJ]	96.3	100.3
Collector efficiency [%]	40.1	41.8
Heat load [MJ]	100.5	
Auxiliary energy [MJ]	19	16.2
Solar fraction [%]	81.5	84.0

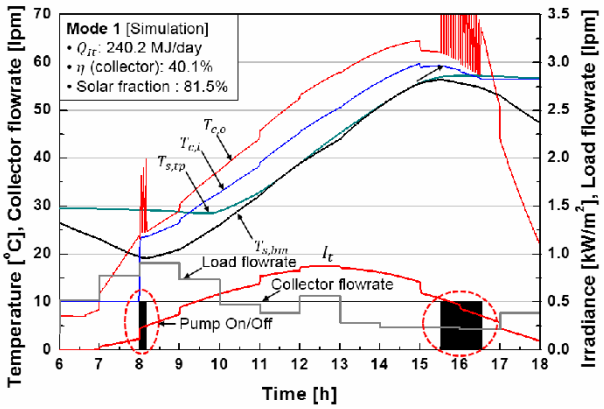

(a) Mode 1

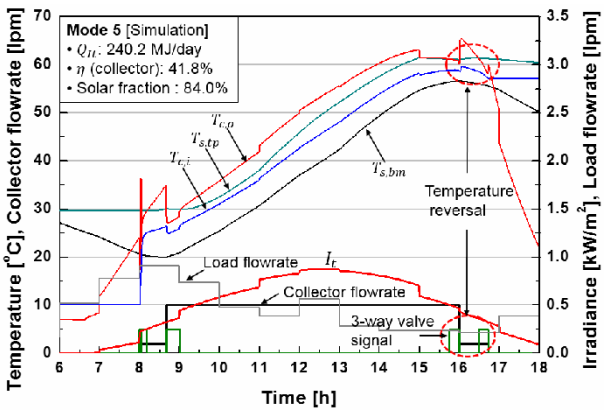

(b) Mode 5

Fig. 11. Daily simulation results of modes 1 and 5.

Figs. 11(a) and (b) show the daily simulation results of modes 1 and 5. In the case of mode 1, shown in Fig. 11(a), the temperature coincidence between the top and bottom inside the storage tank confirmed the fully mixed state (see Fig. 4 for experimental coincidence). Further, the pump operation between sunrise and sunset shows frequent pump ON/OFF transitions. The simulation results of mode 5 revealed the stratified storage tank ($T_{s,tp} - T_{s,bm} > 0$), the temperature reversal (08:00 - 09:00 and 15:30 - 17:00) and the extended operation time (16:30 - 16:45). Those two phenomena can be qualitatively confirmed via experiment in mode 5, as shown in Fig. 8(b).

Simulated results of the collector efficiency were 40.1% (96.3/240.2 MJ) for mode 1 and 41.8% (100.3/240.2 MJ) for

Table 4. Summary of the annual simulation results for the five modes (solar radiation: 52.6 GJ, heat load: 26.2 GJ).

	Mode 1	Mode 2	Mode 3	Mode 4	Mode 5
Collected heat [GJ]	19.0	19.5	19.9	19.6	20.0
Collector efficiency [%]	36.12	37.07	37.83	37.26	38.02
Auxiliary energy [GJ]	9.06	8.56	8.55	8.50	8.49
Solar fraction [%]	65.42	67.33	67.37	67.56	67.60

mode 5. Mode 5 showed slightly improved performance compared to mode 1. Further, the solar fraction of mode 5 (81.5%) was higher than mode 1 (80.4%). The comparison results are summarized in Table 3.

4.4 Comparison of annual simulation results

The annual simulation results of the five modes are summarized in Table 4. Mode 2 shows higher performance compared to mode 1. This result is attributable to the stratification enhanced in mode 2, caused by intensive upper heating. In addition, the performance of mode 3, modes 4 and 5 are all higher than that of mode 2. This suggests that the prevention of temperature reversal and 2-stage flowrate control are effective regarding performance improvement. The results of mode 4 show a slightly improved performance (0.19%p of collector efficiency, 0.23%p of solar fraction) compared to mode 2. Mode 3 collects more heat (19.9 GJ) compared to mode 4 (19.6 GJ), which is also close to the collected heat of mode 5 (20.0 GJ). We conclude that the prevention of temperature reversal is crucial for improvement of the system performance. The annual collector efficiency is 36.12% (19.0/52.6 GJ) for mode 1 and 38.02% (20.0/52.6 GJ) for mode 5. Therefore, mode 5 shows an improved performance (5.26%; (38.02-36.12)/36.12 of collection efficiency) compared to mode 1. In the daily simulation results shown in Table 3, mode 5 shows an increased heat collection (266.3 MJ) compared to mode 1 (252.4 MJ). However, annual simulation shows that the collected heat of mode 4 (19.6 GJ) does not show a significant increase compared to the collected heat of mode 2 (19.5 GJ). It is thought that an increase in the average collector temperature lowers the collector efficiency when the flowrate is low, as seen in Fig. 3. Therefore, the collected heat of mode 4 is lower than that of mode 3. The collector efficiency of mode 3 is slightly higher, 0.57%p more than mode 4, but solar fraction is lower by 0.19%p. From the annual simulation of mode 4, the 2-stage flowrate control is thought to be more effective in terms of solar fraction than the collector efficiency. Overall, mode 5 is the best if all four performances in Table 4 are considered.

5. Conclusions

We examined the system performance of the solar thermal system for a novel improvement method which combines a 2-stage flowrate control and the prevention of the temperature reversal inside the storage tank.

Experimental results showed that the lower heating produces almost perfect mixing inside the storage tank. However, the intensive upper heating definitely builds up the thermal stratification. Temperature reversal easily occurred in the sudden deterioration of irradiation as well as in the late afternoon. This phenomenon also occurred when the load was applied. When an adequately developed control algorithm was applied, a 3-way prevented temperature reversal. Further, this algorithm made it possible for the 2-stage flowrate to extend the solar energy collection time.

The annual simulation showed that the proposed combined method improves the collection efficiency by 1.9%p, and the solar fraction by 2.2%p compared to the conventional lower heating method. Further, 1 GJ of solar energy was additionally collected, which is an improvement of 5.3%.

Acknowledgment

This work was supported by the grant from the National Research Foundation of Korea (NRF), which is supported by the Korean government (MSIP) (No.NRF-2015M3D2A1032826).

Nomenclature

A_c : Collector area [m^2]
C_p : Specific heat of antifreeze [kJ/kg·K]
F_R : Collector's heat removal factor [-]
I_t : Incident radiation [kW]
$\dot{m}$: Flowrate [kg/s]
$\dot{Q}$: Solar energy collection rate [W]
T : Temperature [°C]
U_L : Collector's overall loss coefficient [kJ/hr·m^2·K]

Subscript

a : Atmosphere
bm : Bottom
c : Collector
i : Inlet
low : Low flowrate
nor : Normal flowrate
o : Outlet
s : Storage tank
tp : Top

Greek symbol

α : Absorptance [-]
η : Collector efficiency [-]
τ : Transmittance of collector's cover [-]

References

[1] H. Hong, 3% use of alternative energy in 2006 and solar

thermal system, *J. SAREK,* 33 (2004) 47-54.
[2] I. Dincer and M. A. Rosen, *Thermal Energy Storage – Systems and Application*, Second Ed., John Wiley & Sons, New York, USA (2002).
[3] J. F. Haltiwanger and J. H. Davidson, Discharge of a thermal storage tank using an immersed heat exchanger with an annular baffle, *Solar Energy*, 83 (2009) 193-201.
[4] J. D. Chung, J. H. Park and S. H. Cho, Effect of design factors on the performance of stratified thermal storage tank, *Korean Journal of Air-Conditioning and Refrigeration Engineering*, 16 (11) (2004) 1077-1083.
[5] J. D. Chung, Integral approximate solution for stratified thermal storage tanks considering mixing region, *Proceedings of the SAREK Summer Annual Conference*, Korea (2010) 43-48.
[6] Y. S. Lee, S. N. Lee and J. R. Kim, Effect on stratification due to diffuser shape in a thermal storage tank, *Korean Journal of Air-Conditioning and Refrigeration Engineering*, 17 (11) (2005) 990-997.
[7] A. Musser and W. P. Bahnfleth, Parametric study of charging inlet diffuser performance in stratified chilled water storage tanks with radial diffusers: Part 1-model development and validation, *International Journal of HVAC&R Research*, 107 (2001) 22-407.
[8] H. Han, D. Y. Lee, S. R. Kim, H. J. Kim, J. M. Choi, J. S. Park and S. Kim, Recent progress in air-conditioning and refrigeration research : a review of paper published in the korean journal of air-conditioning and refrigeration engineering in 2012, *Korean Journal of Air-Conditioning and Refrigeration Engineering*, 25 (6) (2013) 346-361.
[9] L. Li, M. Zaheeruddin, S. H. Cho and S. K. Hong, Simulated performance of a combined radiant floor heating and domestic hot water supply system under different control strategies, *International Journal of Air-Conditioning and Refrigeration*, 21 (2) (2013) 1350011.
[10] J. Hu, O. Sari and C. Mahmed, Improving ice formation by additive for cold energy storage, *International Journal of Air-Conditioning and Refrigeration*, 22 (3) (2014) 1450012.
[11] H. S. Son, J. W. Kwon, S. H. Lee, C. Kim and H. Hong, The effect of upper-heating system in solar water storage tank, *International Journal of Air-Conditioning and Refrigeration*, 22 (4) (2014) 1450027.
[12] U. J. Lee, C. Kim and H. Hong, Operation effect of solar thermal storage tank by upper concentrate heating coil, *Proceedings of the SAREK Summer Annual Conference*, Korea (2014) 60-63.
[13] U. J. Lee, C. Kim and H. Hong, Prevention of temperature reversal in upper heating of solar thermal storage tank, *Proceedings of the SAREK Winter Annual Conference*, Korea (2014) 742-745.
[14] D. W. Lee and K. H. Lee, The experimental research for the collecting characteristics of the passive and active type domestic solar hot water systems, *Journal of the Korean Solar Energy Society*, 33 (6) (2013) 12-18.
[15] J. W. Kwon and H. Hong, Enhancement of stratification for solar water storage tank with spiral jacket and coil (Part 1: Verification Experiment), *Korean Journal of Air-Conditioning and Refrigeration Engineering*, 24 (4) (2012) 336-342.
[16] J. A. Duffie and W. A. Beckman, *Solar Engineering of Thermal Processes*, Fourth Ed., John Wiley & Sons, New York, USA (2013).
[17] N. Cardinale, F. Piccininni and P. Stefanizzi, Economic optimization of low-flow solar domestic hot water plants, *Journal of the Renewable Energy*, 28 (12) (2003) 1899-1914.
[18] J. Bang and W. Yoon, Stochastic analysis of a collection process of submicron particles on a single fiber accounting for the changes in flow field due to particle collection, *Journal of Mechanical Science and Technology*, 28 (9) (2014) 3719-3732.
[19] H. S. Son, C. Kim, D. Reindl and H. Hong, The effect of manifold in liquid storage tank applied to solar combisystem, *Journal of Mechanical Science and Technology*, 29 (3) (2015) 1289-1295.

Appendix

In order to acquire the error data between the thermocouple used in this experiment and the standard thermometer (mercury thermometer), we performed a temperature comparison experiment for a total of 150 points (25 points each for 5°C, 10°C, 20°C, 30°C, 40°C, 50°C). The data (standard temperature-thermocouple temperature) are presented in the histogram in Fig. A.1. Statistical analysis shows that the thermocouple temperature is lower than the standard temperature by 0.495°C in the error range of ±0.022°C (confidence level: 95%).

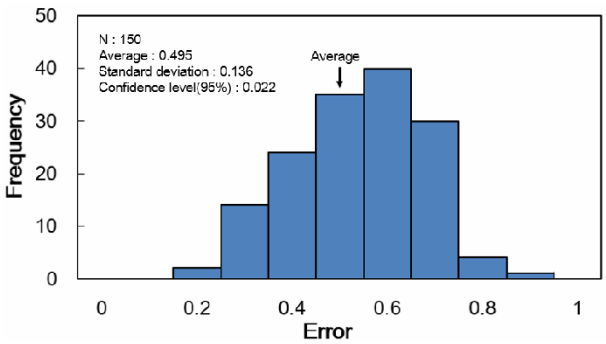

Fig. A.1. Histogram of the temperature error data.

Jong Hyun Kim received his B.S. and M.S. in Aerospace and Mechanical Engineering from Chosun University in 2002, and Kyung Hee University in 2011, respectively. Currently, he is a Ph.D. student at the Department of Mechanical Engineering Kyung Hee University, Yongin, Korea.

Uk Jae Lee received his B.S. and M.S. in Mechanical Engineering from Kyung Hee University in 2013 and 2015, respectively. Currently, he is working for Hyundai Development Company. His research interests are solar thermal system.

Longjie Li received his B.S. degree in Mechanical Engineering from Kyung Hee University in 2012. Currently, he is a M.S. student at the Department of Mechanical Engineering, Kyung Hee University, Yongin, Korea.

Chul Kim received his B.S., M.S. and Ph.D. degrees in Mechanical Engineering from Seoul National University in 1983 and 1985, and Yonsei University in 2010, respectively. Currently, he is an Adjunct Professor at the Department of Mechanical Engineering, Kyung Hee University, Yongin, Korea. His research interests are electro hydrodynamics, CFD and computational neuroscience.

Hiki Hong received his B.S., M.S. and Dr. Eng in Mechanical Engineering from Seoul National University in 1983 and 1986, and Tokyo Institute of Technology in 1993, respectively. Currently, he is a Professor at the Department of Mechanical Engineering, Kyung Hee University, Yongin, Korea. His research interests are solar thermal system, building energy saving and thermal storage.